

Supporting Information

Electrochemical imaging and redox interrogation of surface defects on operating SrTiO₃ photoelectrodes

Burton H. Simpson, Joaquín Rodríguez-López*

Department of Chemistry, University of Illinois at Urbana-Champaign, Urbana, IL, 61801

*Correspondence should be addressed to joaquinr@illinois.edu

Contents

1. SrTiO ₃ Preparation Procedures.....	S2
2. SrTiO ₃ Characterization	S3
3. Electrochemical Measurements.....	S5
4. Numerical Simulations.....	S8

1. SrTiO₃ Preparation Procedures

The as-purchased (100) STO (MTI Corporation, 10x10x1 mm, 1 side polished, made in Japan) was first rinsed thoroughly with acetone, isopropyl alcohol, and Milli-Q water (18.2 MΩ). It was then immersed in 7:1 buffered oxide etch to remove any surface contaminants for 30 seconds before being thoroughly rinsed with Milli-Q water. Following this, the samples were annealed at 1050 °C under a 50 sccm hydrogen flow for 3 hours. The patterns were milled using a FEI Dual Beam 235 FIB. For milling, a gallium metal ion source was used with an accelerating voltage of 30 keV and the milling current was set to 1000 pA. After milling, the buffered oxide etch procedure was repeated to remove any potential contaminants deposited by the electron or ion beam.

2. SrTiO₃ Characterization

Table S1: Calculated dopant density from Mott-Schottky measurements

EIS frequency (Hz)	Slope	E _{fb} (V vs. Ag/AgCl)	R ²	n _D (cm ⁻³)
100	5.42×10 ¹¹	-2.09	0.99993	2.78×10 ²⁰
200	5.50×10 ¹¹	-2.1	0.99991	2.74×10 ²⁰
500	5.58×10 ¹¹	-2.12	0.99992	2.70×10 ²⁰
1000	5.62×10 ¹¹	-2.22	0.99993	2.68×10 ²⁰
1000	5.65×10 ¹¹	-2.24	0.9999	2.66×10 ²⁰

Relative permittivity of STO (ϵ) = 332

$$n_D = 2 / (332 * 8.854e-14 * (\pi * (0.13)^2)^2 * 1.602e-19 * \text{Slope})$$

$$n_{d,avg} = 2.71 \pm 0.05 \times 10^{20} \text{ cm}^{-3}$$

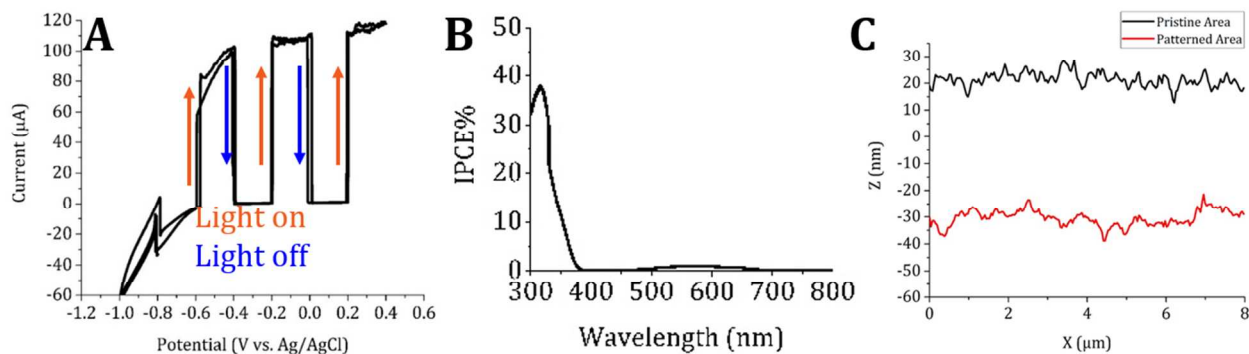


Figure S1: Photoelectrochemical characterization of STO. A) Chopped light voltammogram of STO in 0.1 M borate buffer (pH 9.3). B) IPCE measurements for the prepared STO samples indicate high photoactivity in the UV and some visible light activity. C) AFM linescans of the STO surface comparing a pristine area with a patterned area. The RMS roughness is 2.6 nm for the pristine area, but 3.03 for the FIB patterned area.

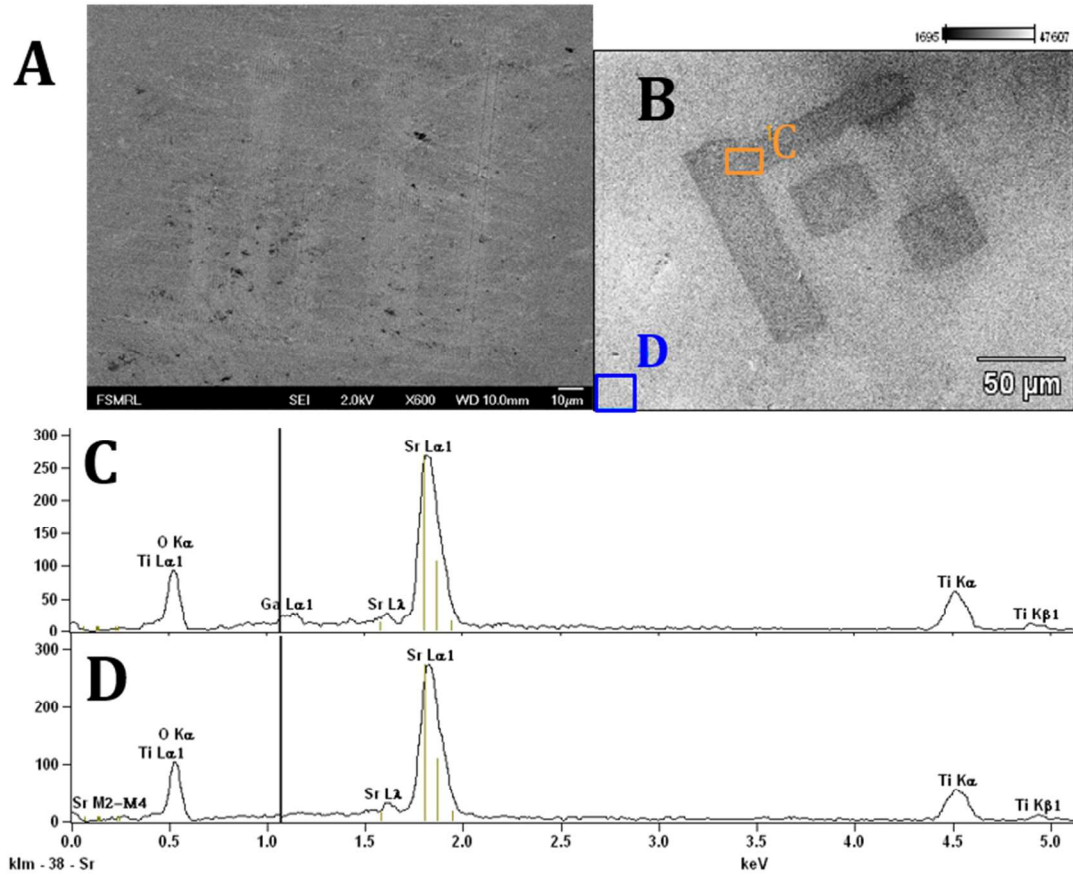


Figure S2: Characterization of FIB-milled areas on STO. A) A low voltage SEM image clearly shows that milled areas produce more secondary electrons than pristine areas, indicating a less n-type character. B-D) The patterns shown in the paper (Fig. 1C) had milled features too small to produce a clearly identifiable gallium signal over the noise levels in energy-dispersive X-ray spectroscopy. We used identical milling parameters to produce the pattern shown in S3B with larger features so that spectra could be collected from larger spots to decrease the relative noise. S3C shows an EDS spectrum taken within this orange box in S3B that has clearly identifiable gallium peaks. In contrast, the EDS spectrum in S3D taken in the blue box in S3B shows no evidence of gallium present on the pristine surface.

3. Electrochemical Measurements

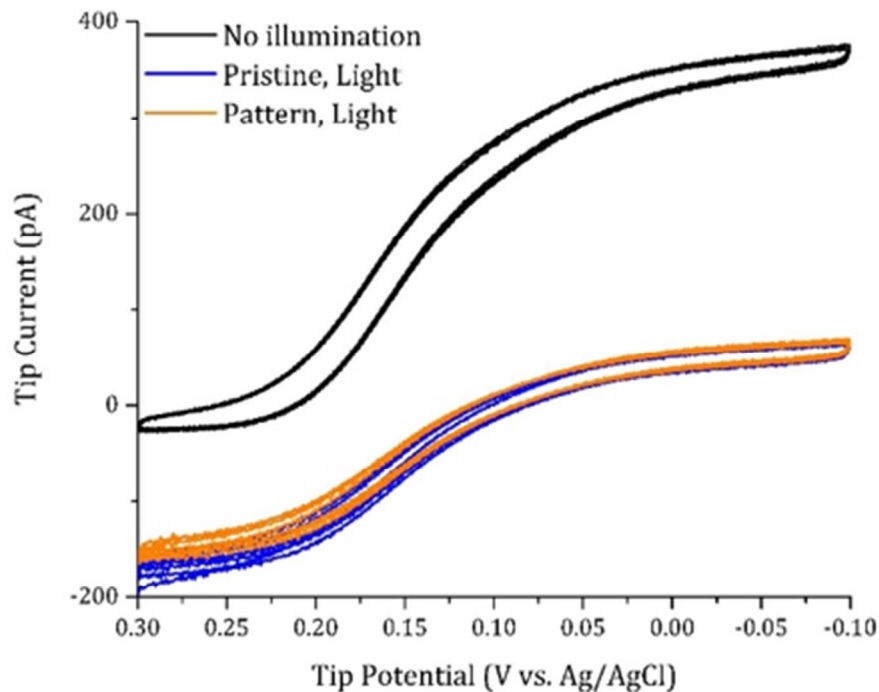


Figure S3: CVs on a C UME ($a = 4 \mu\text{m}$) positioned at $L=1$ over either a pristine or a patterned area in a $50 \mu\text{M}$ solution of $\text{K}_3[\text{Fe}(\text{CN})_6]$ in 100 mM borate buffer ($\text{pH}=9.4$). Without illumination, the reduction of ferricyanide gives a cathodic current. With the substrate illuminated at open circuit, equilibration of the mediator with the substrate converts most of the ferricyanide to ferrocyanide, and a CV in the same potential range shows a primarily anodic current. The anodic current measured over the pristine surface is slightly larger due to the higher activity of the pristine surface.

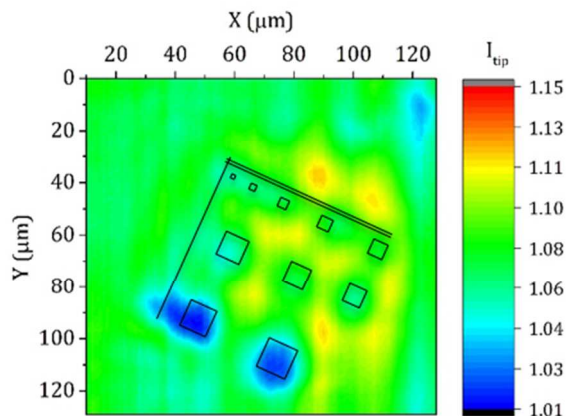


Figure S4: Figure 2E after a linear correction to account for current drift was applied. For this technique, we found the slope of current change with respect to x and y independently, then subtracted these increases from the original image data. The first 10 lines scanned were removed for this image to enhance contrast of the other regions. The original image showed highest positive feedback in the bottom right corner. This SECM image was taken with the substrate illuminated at open circuit using a carbon UME ($a = 4 \mu\text{m}$) positioned at $L=1$ and biased to reduce 0.6mM O_2 and 0.1 M TBA.PF_6 in DMF.

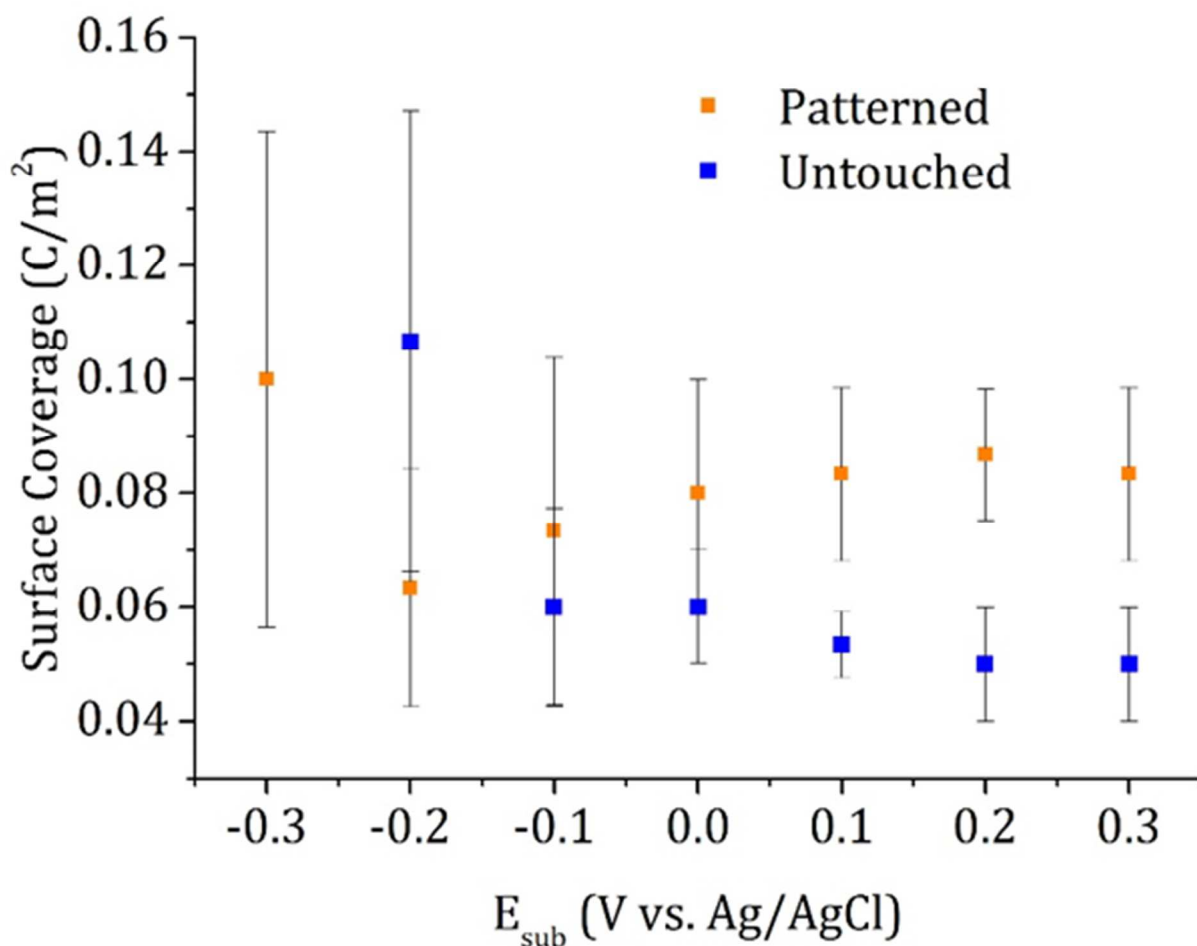


Figure S5: Measured surface coverage of ROS formed on STO during photoassisted water oxidation at a series of substrate potentials. At minimally activating potentials, the surface coverage is unreliable, but as the potential increases, the surface reaches a limiting coverage. Surface coverages were extracted by fitting experimental transients to simulated surface interrogations.

4. Numerical Simulations

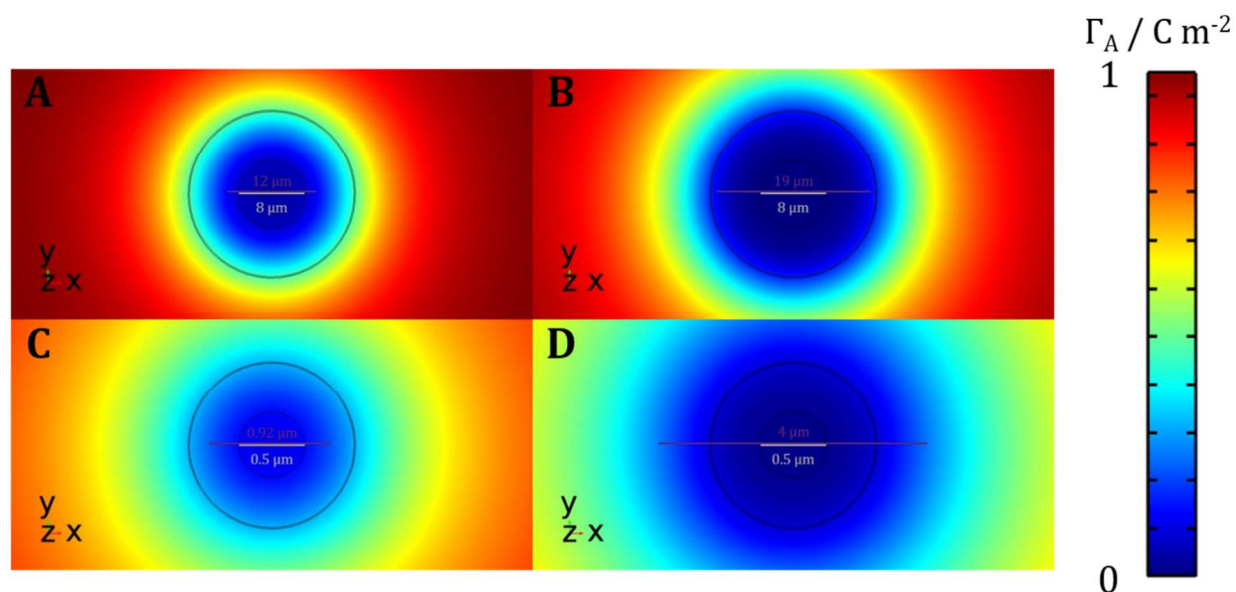


Figure S6: Simulated surface coverage (Γ_A) of reactive adsorbates after surface interrogations using (A and B) a 4 μm radius UME or (C and D) a 240 nm radius nanoelectrode. Simulations used parameters relevant to experimental conditions: [mediator]=50 μM , $D=7.0 \times 10^{-10} \text{ m}^2/\text{s}$. Γ_A and k_{si} were chosen from values that best fit SI-SECM data taken with the $a=240 \text{ nm}$ electrode.